Available online at www.sciencedirect.com
SCIENCE DIRECT®
Composite Structures 64 (2004) 63–69
COMPOSITE STRUCTURES
www.elsevier.com/locate/compstruct

Shear buckling of a composite drive shaft under torsion

Mahmood M. Shokrieh [a,*], Akbar Hasani [a], Larry B. Lessard [b]

[a] *Composites Research Laboratory, Mechanical Engineering Department, Iran University of Science and Technology, Narmak, Tehran 16844, Iran*

[b] *Mechanical Engineering Department, McGill University, 817 Sherbrooke St.W., Montreal, Qc, Canada H3A 2K6*

Abstract

In this research the torsional stability of a composite drive shaft torsion is studied. Composite materials are considered as the suitable choice for manufacturing long drive shafts. The applications of this kind of drive shafts are developed in various products such as cars, helicopters, cooling towers, etc.

From the design point of view, local and global torsional instability of drive shafts limits the capability for them to transfer torque. After reviewing the closed form solution methods to calculate the buckling torque of composite drive shafts, a finite element analysis is performed to study their behavior. Furthermore, to evaluate the results obtained by the finite element method, a comparison with experimental and analytical results is presented. A case study of the effects of boundary conditions, fiber orientation and stacking sequence on the mechanical behavior of composite drive shafts is also performed.

Finally, the reduction of the torsional natural frequency of a composite drive shaft due to an increase of applied torque is studied.

Keywords: Composite drive shafts; Finite element analysis; Buckling

1. Introduction

The general stability of drive shafts under torsion has been studied by many researchers. Greenhill [1] for the first time in 1883 presented a solution for torsional stability of long solid shafts. This method of solution can be extended for calculating of the first torsional buckling mode of a hollow shaft. The first and oldest buckling analysis of thin-walled cylinders under torsion was presented by Schwerin [2] in 1924. However, his analysis did not show a good agreement with experimental results.

In 1931 Kubo and Sezawa [3] presented a theory for calculating the torsional buckling of tubes and also reported on experimental results for rubber models. However, this theory did not show an agreement with experimental results. Lundquist [4] performed extensive experiments on the strength of aluminum shafts under torsion reported in 1932.

There was still no analytical solution until 1933 for simulation of the buckling behavior of drive shafts, so experimental results were the only basis for the research of Donell [5]. In 1934 he presented a theoretical solution for the instability of drive shafts under torsion. He used the theory of thin-wall shells for analysis and evaluated his theory with available experimental results, which included about fifty tests. These studies showed that the torsional failure load measured by experiments is always less than that obtained by theory. The main reason is the initial eccentricity of the shafts in the experiments. All of the above mentioned researchers were limited their research to isotropic materials.

A general theory for isotropic shells was presented for the first time by Ambartsumyan [6] and Dong et al. [7] in 1964. Ho and Cheng [8] performed a general analysis on the buckling of non-homogeneous anisotropic thin-wall cylinders under combined axial, radial and torsional loads by considering four boundary conditions. Chehil and Cheng [9] studied the elastic buckling of composite thin-wall shell cylinders under torsion based on the large deflection theory of shells.

Tennyson [10] using a theoretical method studied the classical linear elastic buckling of non-isotropic composite cylinders, ''perfect'' and ''imperfect'', under different loading conditions. He compared his results with experiments. Bauchau and Krafchack [11] in 1988

* Corresponding author. Fax: +98-21-200-0016.
E-mail address: shokrieh@iust.ac.ir (M.M. Shokrieh).

0263-8223/$ - see front matter © 2003 Elsevier Ltd. All rights reserved.
doi:10.1016/S0263-8223(03)00214-9

measured the torsional buckling load of some composite drive shafts made of carbon/epoxy. They predicated the torsional buckling load using shell theory and by considering the effects of elastic coupling and transverse shear deformation.

Bert and Kim [12] in 1995 performed a theoretical analysis on torsional buckling of composite drive shafts. They predicated the torsional buckling load of composite drive shafts with various lay-ups with good accuracy by considering the effect of off-axis stiffness and flexural moment. This theory can predict the torsional buckling of composite drive shafts under pure torsion and combined torsion and bending.

Chen and Peng [13] in 1998, using a finite element method, studied the stability of composite shafts under rotation and axial comparison load. They predicated the critical axial load of a thin-wall composite shaft under rotation.

2. Problem statement

When a hollow shaft is subjected to torsion, at a certain amount of torsional load instability occurs. This is called the torsional buckling load. Therefore, the torsional buckling load is important in the design of drive shafts. This parameter is even more critical in the design of composite shafts, because composite drive shafts are often made longer. Although increasing the length of drive shaft does not change the static torsional stress, it can decrease the torsional buckling load capacity of the shafts. Therefore, the calculation of the torsional buckling load for composite drive shafts is very important. In the following section it is shown that the design must be such that the torsional buckling strength of a shaft must be higher than the static torsional strength.

Second, the stacking sequence of the layers affects the torsional buckling capacity of drive shafts. Therefore, selection a suitable stacking sequence can increase the torsional buckling load of the composite shafts.

Thirdly, in general composite drive shafts have a lower torsional buckling capacity in comparison with metallic shafts for the same geometry. An important reason is the existence of interlaminar shear stresses and the coupling between the in-plane and out-of-plane stresses for composite shafts. In a metallic shaft under torsion, the shear stress is the only existing stress, however, for a composite shaft all stresses can exist.

3. Analytical relations to calculate the torsional buckling load of composite shafts

In the design of a composite shaft, before applying a finite element technique, a closed form solution is useful. In order to have an order-of-magnitude solution for a design, a simple equation is needed to calculation the torsional buckling load of long thin-wall shafts. There are various existing equations for this purpose in the literature. These equations are empirical, obtained based on experimental studies. In the following, two equations used by many researchers are presented. The first equation was presented in Ref. [14].

$$T_{\text{buckling}} = \frac{2.289}{\sqrt{L}} \times E_1^{0.375} \times E_2^{0.625} \times t^{2.25} \times D^{1.25} \tag{1}$$

The second equation was presented in Ref. [15].

$$T_{\text{buckling}} = \frac{1.854}{\sqrt{L}} \times E_1^{0.375} \times E_2^{0.625} \times t^{2.25} \times D^{1.25} \tag{2}$$

In these equations, t is the thickness, D is the average diameter, L is the length of the shaft and E_1 and E_2 are the longitudinal and transverse stiffness of the shaft, respectively.

Based on these equations, the torsional buckling load is maximized for a 45° orientation of fibers, with E_1 and E_2 equal. Suppose the stiffness of the composite material is similar to that of the steel, i.e., 200 GPa. Then, for a 45° orientation of fibers, the longitudinal and transverse stiffness (E_1 and E_2) of the composite shaft would be much less than 200 GPa. This shows that if a metallic shaft is replaced by a composite shaft (with the same geometry), the thickness of the composite shaft must be larger. To obtain a similar torsional buckling load for both shafts, the thickness of the composite shaft must be increased. By considering the low density of composites, this does not significantly increase the weight of the composite shafts.

4. Finite element analysis to calculate the torsional buckling load of composite shafts

In this research, finite element analysis is performed using ANSYS software. To model the composite shaft, the shell 99 element is used and the shaft is subjected to torsion. The shaft is fixed at one end in axial, radial and tangential directions and is subjected to torsion at the other end. After performing a static analysis of the shaft, the stresses are saved in a file to calculate the buckling load. The output of the buckling analysis is a load coefficient which is the ratio of the buckling load to the static load. This software also calculates the modes of buckling of the composite shaft. In Figs. 1 and 2, the mesh configuration and the first and the second modes of buckling of the composite shaft are shown.

In Table 1, the results of the buckling torque obtained from closed form solution are shown. Finite element analysis and experimental results are compared. The results are presented for carbon/epoxy composite shafts with different ply sequences and the material properties

Fig. 1. First mode of torsional buckling of the composite shaft.

Fig. 2. Second mode of torsional buckling of the composite shaft.

that are shown in Table 2. From Table 1, two important points can be made. First, the ply sequence has an important effect on the torsional buckling of the shaft. Second, the results obtained from finite element analysis in this research show good agreement with experimental results. In most cases, the results obtained by this research show a better agreement with experimental results compared with the closed form methods presented in [11,12].

5. Effect of parameters on torsional buckling load of composite shafts

In design of composite shafts, the effect of fiber orientation on torsional buckling load must be considered. In Table 3, the effect of fiber orientation on the torsional buckling load of a composite shaft is presented. In this table, the results presented by Ref. [12] and the finite element analysis performed in this research are compared. The mechanical properties of the composite materials are show in Table 4.

There are some differences between the results obtained in this research and the results from Ref. [12], however, as shown in Table 3, the results obtained from the two methods are in good agreement. By comparing these results with experimental results in Table 3, it is clear that the result obtained in this research show better agreement with experimental results. The boundary condition at each end of the shaft has a minor effect on the torsional buckling load [12]. To clarify this postulation, a boron/epoxy composite drive shaft with four different boundary conditions is analyzed [12] and the results are presented in Table 5.

6. Comparison between finite element and analytical methods

To evaluate the accuracy of Eqs. (1) and (2), the torsional buckling load of a shaft is calculated using these equations. The results are compared with results obtained by finite element methods. The mechanical properties of the material and the geometry of the shaft are summarized in Table 6.

Table 1
Buckling analysis of composite shafts

Shaft no.	Lay-up definition	L (m)	R (mm)	Buckling torque (N m)			
				a*	b*	c*	d*
1	15, −15, −45, −15, 15, +45	0.26	41.27	486	523	535	472
2	−45, −15, 15, 45, 15, −15	0.26	41.27	350	366	382	372
3	30, −30, 30, −30, 30, −30	0.32	37.19	390	535	394	395
4	45, −45, 45, −45, 45, −45	0.32	37.42	490	490	540	460
5	0, 0, 45, −45, 45, −45, 0, 0	0.32	37.42	543	540	671	670

a*: Experimental result from Ref. [11].
b*: Theoretical prediction for simply supported edges from Ref. [11].
c*: Sanders thin shell theory from Ref. [12].
d*: Present prediction using ANSYS software.

Table 2
Mechanical properties of carbon/epoxy

$E_{xx} = 134$ GPa	$G_{xy} = 4.6$ GPa
$E_{yy} = 8.5$ GPa	$v_{xy} = 0.29$
Layer thickness = 0.1334 mm	

Using Eq. (1):

$$T_{\text{buckling}} = \frac{2.289}{\sqrt{1.56}} \times (102 \times 10^9)^{0.375} \times (8.56 \times 10^9)^{0.625} \times (0.003)^{2.25} \times (0.07)^{1.25}$$

$$T_{\text{buckling}} = 3000 \text{ N m}$$

Using Eq. (2):

$$T_{\text{buckling}} = \frac{1.854}{\sqrt{1.56}} \times (102 \times 10^9)^{0.375} \times (8.56 \times 10^9)^{0.625} \times (0.003)^{2.25} \times (0.07)^{1.25}$$

$$T_{\text{buckling}} = 2440 \text{ N m}$$

As shown in Table 7, Eq. (2) shows more accuracy for predicting the torsional buckling load of a composite shaft. Therefore, this equation is used for further calculations in this research.

7. Variation of torsional natural frequency of a shaft due to applied torque

The buckling of a shaft under torsion is similar to buckling of a shaft under axial load from a mathematical point of view. In a composite shaft, the torsion load creates shear and compression stresses in the layers in the on-axis direction.

Another definition of axial buckling force of a shaft is the load on which the first natural frequency of the shaft becomes zero. In other words, when a beam is subjected to axial load, the first natural frequency of the first bending mode is decreased by increasing the load. For a certain amount of axial load, the magnitude of first natural frequency reaches zero. In fact, for this very reason the first natural torsional frequency of a shaft must be higher than the first natural bending frequency of that same shaft. In this way, when the shaft is under the applied torque, the natural torsional frequency of the shaft does not become less than the natural bending frequency. Normally, the critical speed of the shaft is selected based on the first natural bending frequency.

Table 4
Mechanical properties of the composite shaft

Layer thickness	0.132 mm
Number of layers	10
Length	2.47 m
Average diameter	12.57 cm
Longitudinal stiffness	211 GPa
Transverse stiffness	24.1 GPa
Shear stiffness	6.89 GPa
Poisson's ratio	0.36

The square of the natural frequency of a structure is a linear function of the applied load. This means that by increasing the axial load, the square of natural frequency decreases linearly [16]. There is a similar behavior for a shaft under torsion. In the following, using some assumptions, this phenomenon is shown.

A structure is considered with stiffness $[k]$, geometrical stiffness $[k_g]$, and the mass matrix $[M]$. It must be mentioned that the geometrical stiffness is calculated for a unit load and changes linearly with the load. To calculate the natural frequency of a structure under load, the following eigenvalue problem should be solved:

$$\left[[k] + \lambda[k_g] - \omega^2[M]\right]\{a\} = 0 \tag{3}$$

In which, λ is a known parameter and showing the magnitude of loading and ω is unknown. Eq. (3) can be written as follows:

$$\left[[k] + \alpha\lambda_{cr}[k_g] - \omega^2[M]\right]\{a\} = 0 \tag{4}$$

and $0 \leqslant \alpha \leqslant 1$. Eq. (4) is written as follows:

$$\left[(1-\alpha)[k] + \alpha([k] + \lambda_{cr}[k_g]) - \omega^2[M]\right]\{a\} = 0 \tag{5}$$

By assuming that the mode shapes of bending and torsion are the same, the second term of Eq. (5) vanishes and we have:

$$\left[(1-\alpha)[k] - \omega^2[M]\right]\{a\} = 0 \tag{6}$$

$$\left[[k] - \frac{\omega^2}{(1-\alpha)}[M]\right]\{a\} = 0 \tag{7}$$

Eqs. (6) and (7) show that, for a structure with similar mode shapes for bending and torsion, the square of the natural frequency is a linear function of the load and under critical load, one of the natural frequencies becomes zero.

In Fig. 3, the variation of the square of the natural frequency of a beam as a function of the load is shown. As shown in this figure, the square of the natural frequency does not depend on the boundary conditions

Table 3
Variation of torsional buckling load with fiber orientation

Ply orientation angle (degree)		0	15	30	45	60	75	90
Buckling torque (N m)	Ref. [12]	587	974	1126	1790	2617	3156	3016
	Present research	2100	1984	1320	1550	2140	2793	2950

Table 5
Torsional buckling load of a boron/epoxy composite drive shaft with four boundary conditions using Sander's shell theory

Boundary condition	Buckling torque (N m)
(1) Simply supported at both ends without axial constraint (freely supported)	3481
(2) Simply supported at both ends with axial constant	3664
(3) Clamped at both ends	3665
(4) Clamped end simply supported	3561

Table 6
Mechanical properties and geometry of a composite shaft

$E_{xx} = 102$ GPa	$t = 3$ mm	$r_m = 0.035$ m
$E_{yy} = 8.56$ GPa	$L = 1.56$ m	$D = 0.07$ m

Table 7
Comparison of analytical and finite element methods

Buckling torque (N m)		
Eq. (1)	Eq. (2)	FEM
3000	2440	2400

and changes linearly by increasing the load and becomes zero as load reaches to critical load. It must be mentioned that the higher natural frequencies also decrease linearly with the axial load. However, only the first natural frequency reaches zero at critical load while the others decrease. All the points mentioned here for a beam under bending are valid for a shaft under torsion.

To examine this phenomenon further, the variation of the first five natural frequencies of a composite shaft in terms of the variation of the applied torque is shown in Figs. 4 and 5. These curves are drawn based on a finite element analysis. The mechanical properties and the geometry of the model are summarized in Tables 8

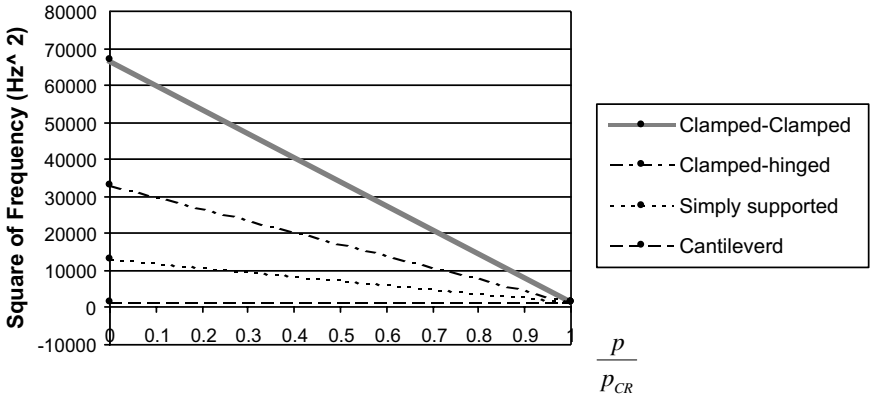

Fig. 3. Variation of squared natural frequency of a beam with different boundary conditions under axial compressive load [16].

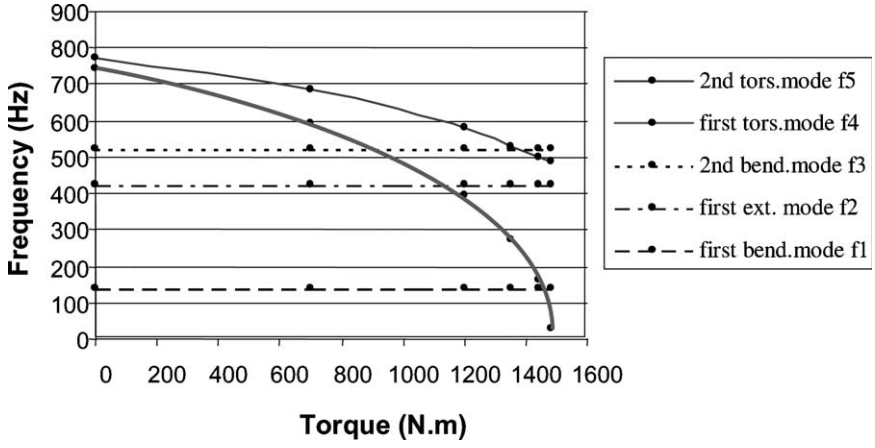

Fig. 4. Variation of the first five natural frequencies of a composite shaft in terms of the applied torque.

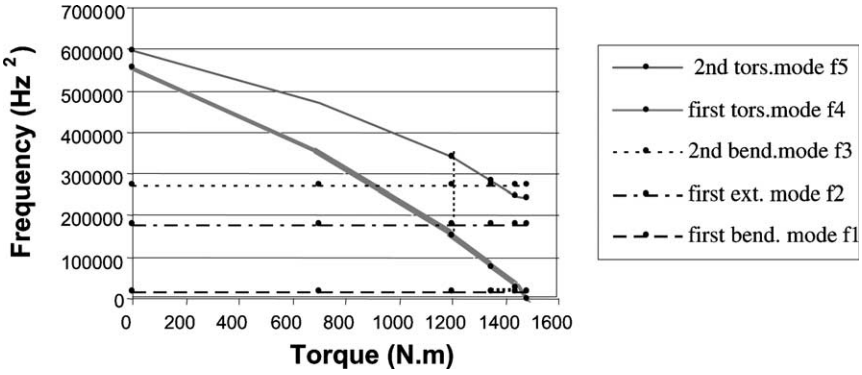

Fig. 5. Variation of the squared first five natural frequencies of a composite shaft in terms of the applied torque.

Table 8
Geometry and fiber volume fraction of the composite shaft

Shaft geometry	Fiber volume fraction	Fiber orientation
$L = 1337$ mm	30% E-glass/epoxy	11°
$t = 2.5$ mm	70% Hs-carbon/epoxy	11°
$D = 63.7$ mm		

Table 9
Material properties of the composite shaft

Material	E_{xx} (GPa)	E_{yy} (GPa)	G_{xy} (GPa)	v	ρ (kg/m^3)
E-glass/epoxy	50	12	5.6	0.3	2000
Hs-carbon/epoxy	134	7	5.8	0.3	1600

and 9. In Figs. 4 and 5, f1 to f5 represent the magnitudes of first natural frequencies of the shaft.

As shown in Fig. 4, if we apply a torque equal to 890 N m the fourth mode of vibration is replaced by the third mode. By increasing the applied torque, the lower modes of vibration are replaced by the higher ones. For a torque equal to 1450 N m, the first frequency of torsion (fourth mode) is equal to the first frequency of bending (first mode). Finally, in a torque equal to 1510 N m, the first natural frequency reaches to zero and the shaft is unstable at that point.

In Fig. 5, the fairly linear variation of the square of the natural frequencies in terms of the applied torque is shown. This linear variation verifies the results obtained by finite element technique. The results obtained by the present research show that in design of a composite shaft, the buckling torque must be properly higher than the static applied torque.

8. Discussion and results

The results obtained from analysis show that by using finite element analysis, the strength of a composite drive shaft can be simulated. In this research, the effect of boundary conditions and the stacking sequence of the composite layers on the strength of the drive shaft is studied. It is shown that increasing of the applied torque on the shaft reduces the natural frequency. The results obtained in this research are summarized in the following:

- The boundary conditions of the shaft do not have much effect on the buckling torque.
- The fiber orientation of a composite shaft strongly affects the buckling torque.
- The stacking sequence of the layers for a composite shaft also strongly affects the bucking torque.
- The finite element modeling presented in this analysis is able to predict the buckling torque.
- By increasing the applied torque on a shaft, the square of the natural frequencies decrease linearly.
- Increasing the applied torque decreases the natural frequencies of torsion and does not change the other modes.
- The frequency of the first mode of torsion under a certain torque is when the buckling torque becomes zero.

References

[1] Greenhill AG. On the strength of shafting when exposed both to torsion and to end thrust. In: Proc Instn Mech Engrs, London; 1883. p. 182.
[2] Schwerin E. Torsional stability of thin-walled tubes. In: Proceedings of the First International Congress for Applied Mechanics, Delf, The Netherlands; 1924. p. 255–65.
[3] Sezawa K, Kubo K. The buckling of a cylindrical shell under torsion. Aero Research Inst, Tokyo Imperial University, Report No. 176; 1931.
[4] Lundquist E. Strength tests on thin-walled duralumin cylinders in torsion. NACA No. 427; 1932.
[5] Donnell LH. Stability of thin-walled tubes under torsion. NACA Report 479; 1934. p. 95–115.
[6] Ambartsumyan SA. Theory of anisotropic shells. TT F-118, NASA; 1964. p. 18–60.

[7] Dong SB, Pister KS, Taylor RL. On the theory of laminated anisotropic shells and plates. J Aerospace Sci 1962:969–75.
[8] Ho BPC, Cheng S. Some problems in stability of heterogeneous aeolotropic cylindrical shells under combined loading. J AIAA 1963;12:1603–7.
[9] Chehil DS, Cheng S. Elastic buckling of composite cylindrical shells under torsion. J Spacecraft Rockets 1968;5:973–8.
[10] Tennyson RC. Buckling of laminated composite cylinders: a review. J Compos 1975;6:17–24.
[11] Bauchau OA, Krafchack TM, Hayes JF. Torsional buckling analysis and damage tolerance of graphite/epoxy shaft. J Compos Mater 1988;22:258–70.
[12] Bert CW, Kim CD. Analysis of buckling hollow laminated composite drive shafts. Compos Sci Technol 1995;53:343–51.
[13] Chen LW, Kung Peng W. The stability behavior of rotating composite shafts under axial compressive loads. Compos Struct 1998;41:253–63.
[14] Spencer B, McGee J. Design methodology for a composite drive shaft. Advanced composite material, Lincon, NE, USA; 1985. p. 69–82.
[15] The use of continuous fiber composites in drive shafts. Available from: http://www.addax.com/SAE Paper.htm. Addax, Inc.; 1997.
[16] Cook RD, Malkus DS, Plesha ME. Concepts and application of finite element analysis. 3rd ed. John Wiley; 1989.